ELSEVIER

Mercury adsorption by montmorillonite and vermiculite: a combined XRD, TG-MS, and EXAFS study

M.F. Brigatti[a],*, S. Colonna[b], D. Malferrari[a], L. Medici[c], L. Poppi[a]

[a]*Dipartimento di Scienze della Terra, Università di Modena e Reggio Emilia, via Largo S. Eufemia 19, I-41100 Modena, Italy*
[b]*ISM-CNR, Via del Fosso del Cavaliere 100, 00133 Rome, Italy*
[c]*IMAA-CNR, Area della Ricerca di Potenza, Via S. Loja, 85050-Tito Scalo, Potenza, Italy*

Abstract

Synchrotron-based extended X-ray absorption fine structure spectroscopy (EXAFS), X-ray diffraction at room and high temperature, thermal analyses combined with mass spectrometry of evolved gas, and chemical analyses contributed to assess the influence of mercury on montmorillonite and vermiculite layers.

The adsorbed Hg amount was higher for montmorillonite (Hg=37.7 meq/100 g) than for vermiculite (Hg=28.0 meq/100 g). The basal spacing for the Hg treated samples was 15.2 (montmorillonite) and 14.5 Å (vermiculite). Thermal and evolved gas spectrometry analyses suggest that Hg was released at $T \cong 230$ °C and at 600 °C for montmorillonite, but at 550, 800 and 860 °C for vermiculite.

The effect of temperature on Hg release is also apparent when the basal spacing at 230 °C for montmorillonite (d_{001}=10.3 Å) is compared to that for vermiculite (d_{001}=11.8 Å).

EXAFS analyses provide qualitative evidence that oxygen atoms occupy the first coordination shell of Hg in both clay minerals. The best fit between observed and calculated spectra is obtained when montroydite is assumed as a reference model compound.

© 2004 Elsevier B.V. All rights reserved.

1. Introduction

Mercury is one of the most serious contaminants in water and sediment. Even if present in traces, its high toxicity makes it an environmental threat in industrial, mining, and domestic wastes (Lindqvist, 1991; Watras and Huckabee, 1994; Hudson et al., 1995; Watras et al., 2000; Covelli et al., 2001). Hg presents

* Corresponding author. Tel.: +39 59 2055805; fax: +39 59 2055887.

E-mail address: brigatti@unimo.it (M.F. Brigatti).

three valence states (I, II, and 0) which can be readily inter-converted or complexed by organic matter in sediments, making Hg behaviour very complex to predict. Fine-particle materials that present a large surface area such as oxides, oxyhydroxides and layer silicates are among the principal sorbents of the metal species (Collins et al., 1999). Thus, sorption, diffusion and precipitation reactions at the mineral–water interface can significantly retard the release of metal ions into the geosphere (Bothner et al., 1980; Gagnon et al., 1997).

The knowledge of the heavy metal binding to the mineral structure is of fundamental importance to predict the mobility and long-term behaviour of heavy metals in natural systems. A good example is provided by the interaction of Hg solution with goethite surface. The distance between Hg and the two closest oxygen atoms in the mineral is 2.04 Å and the distance between Hg and Fe is 3.28 Å (Collins et al., 1999). Further structural studies dealing with interactions between Hg and minerals like Fe- and Al-(hydr)oxides were carried out by Kim et al. (2004). These authors demonstrated that the presence of sulphate in solution significantly affected Hg(II) sorption, whereas occurrence of chloride resulted in reduced Hg(II). Behra et al. (2001) also supported these conclusions starting from a spectroscopic evidence of the formation of a surface complex between S^{-1} and Hg^{2+}. Due to surface reactivity and large surface area, adsorption and/or exchange of mercury ions to 2:1 clay minerals, such as montmorillonite and vermiculite, is believed to be important in affecting the metal mobility in the environment. The different layer charge value and location in montmorillonite and vermiculite is expected to affect metal sorption as well as stereochemistry of sorbed species. The location of the layer charge determines the strength of the Lewis base: montmorillonite which presents relevant octahedral substitutions behaves as a soft base, whereas vermiculite, mostly characterized by tetrahedral substitutions behaves as a hard base. Hg is a soft Lewis acid, and therefore should prefer the soft montmorillonite layer.

In this paper, a multi-technical approach including EXAFS spectroscopy was used to characterize Hg adsorbed species on 2:1 layer expanding clays with different value and location of the layer charge (i.e., montmorillonite and vermiculite).

2. Materials and methods

2.1. Samples

Samples used were montmorillonite, reference clay STx-1, from Gonzales County, TX, USA (nominal Cation Exchange Capacity, CEC=84.4 meq/100 g) and vermiculite from Bikita (Zimbabwe). Montmorillonite derives its layer charge mostly from low-charge cations sited in the octahedral sheet, whereas the vermiculite layer charge is mostly ascribed to Al for Si tetrahedral substitutions. Details of the mineralogical, chemical and surface properties of montmorillonite under examination can be found in van Olphen and Fripiat (1979) and Costanzo and Guggenheim (2001). Vermiculite sample (mean crystal dimensions $0.1 \times 0.1 \times 0.05$ mm) was analysed chemically, using a wavelength-dispersive ARL-SEMQ electron microprobe (operating conditions: 15 kV accelerating voltage, 15 nA sample current and enlarged spot size of about 8 μm to reduce the damage of the mineral; analyses and data reductions were performed using the Probe software package of Donovan, 1995). The structural formula obtained by averaging chemical data from several crystals is $(Si_{6.19}Al_{1.81})(Fe^{3+}_{0.60}Mg_{5.38}Mn_{0.01}Ti_{0.01})(Mg_{0.52}Ca_{0.05}Na_{0.04}K_{0.01})O_{20}(OH,F)_4$. A tetrahedral layer charge of -1.81 electrostatic valence units (evu), an octahedral layer charge of $+0.62$ evu and a CEC of 142 meq/100 g characterize the vermiculite sample. Vermiculite cell dimensions (determined on the basis of a monoclinic cell; *least square* program LATCOREF; Allmann, 1984) are: $a=5.346(2)$ Å, $b=9.257(2)$ Å; $c=29.044(7)$ Å, $\beta=96.93(2)°$.

Before performing treatments with Hg solutions, a fixed amount of each sample (50 g) was ultrasonified, and the <2-μm size fraction was separated by sedimentation (Jackson, 1975). Afterwards, both montmorillonite and vermiculite samples were air-dried.

2.2. Solutions

According to theoretical calculation, performed from MINTEQA2 program (Allison et al., 1991), Hg phases from 0.01 M $Hg(NO_3)_2$ solution precipitate at pH higher than 2.4 (Fig. 1). Most of the Hg species in solution are Hg^{2+}, $Hg(NO_3)^+$ and $Hg(OH)_2$. At pH=2.4, most of the Hg precipitates as HgO and only small amounts of Hg^{2+}, $Hg(OH)_2$ and $Hg(OH)^+$ are maintained in solution.

The Hg(II) 0.01 M stock aqueous solution used for all treatments was thus obtained from the dissolution of $Hg(NO_3)_2 \cdot 7H_2O$ analytical grade reagent (declared impurity of less than 0.1%) and acidified with nitric acid until pH 2.0 to avoid Hg precipitation.
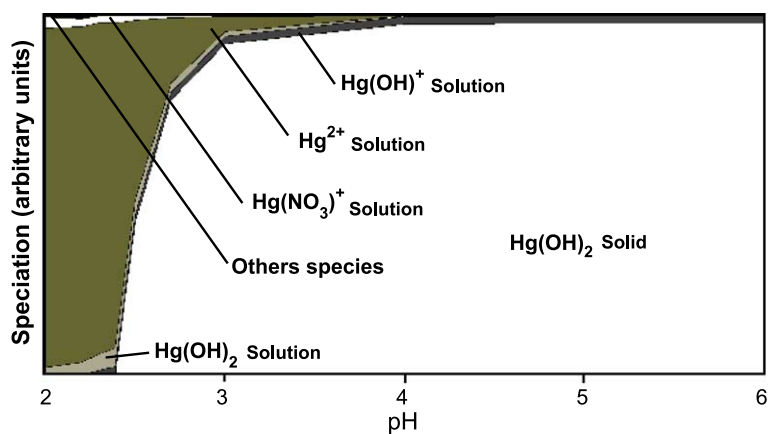
Fig. 1. Relevant Hg species vs. pH for $Hg(NO_3)_2$ 0.01 M solution.

2.3. Hg sorption procedures

Hg-rich expanding phyllosilicates were prepared by mixing 10 g of each smectite sample with 250 ml of Hg(II) 0.01 M solution. The suspensions were stirred for a week at room temperature; pH was monitored continuously by pH-meter (Jenway 3310) equipped with a glass electrode and kept at value lower than 2.2 adding a few drops of concentrated nitric acid. The solutions were then aspirated off, replaced by fresh solutions and the sequence was repeated for another week. Finally, salt in excess was removed from the homoionic clays by dialysis until the aspirated solution tested negative with $AgNO_3$. Filtrates were analysed by atomic absorption spectrophotometry to check for the presence of metal cations used in the exchange.

2.4. Characterization procedures

An atomic absorption spectrophotometer (Varian Spectr AA 300) equipped with cold vapour generator (VGA-76) was used to analyse the amount of metal retained. A well-known amount of each Hg-treated phyllosilicates was digested by nitric-hydrofluoric acid. To stabilize the Hg(II) ions, a 3% (w/w) HNO_3 solution containing 0.05% (w/w) $K_2Cr_2O_7$ was used. The mercury cold vapour generator is a reaction cell where solution under analysis reacts with an acid solution (i.e., 5 M HCl) and a reducing solution (i.e., 0.3% $NaBH_4$ aqueous solution). The equipment is based on the segmented-flow principle derived by Haase et al. (1998). All the previously introduced solutions were separately injected in the reaction cell through a piping system by a peristaltic pump. In the reaction cell, Hg was reduced to atomic Hg^0 and vaporized. Finally, Hg^0 was transferred to the absorption cell (a quartz tube, length 180 mm, diameter 8 mm) where the absorbance was measured at 253.7 nm. The detector consisting of a photomultiplier and an interference filter was optimised for the 253.7 nm line. Peak height measurements were performed by the software of the spectrophotometer.

The basal d spacing was determined by X-ray powder diffraction (XRD) analysis at room temperature (T=25 °C, relative humidity (RH)=60%) and in the temperature range 25≤T (°C)≤450, on oriented mounts, using a Philips PW 1729 diffractometer (CuKα radiation; quartz as standard) equipped with a monochromator and an in situ heating apparatus.

Thermal analyses were performed using a Seiko SSC 5200 thermal analyser equipped with a quadrupole mass spectrometer (ESS, GeneSys Quadstar 422) to analyse the gases evolved during thermal reactions. Gas sampling by the spectrometer was performed via an inert, fused silicon capillary system, heated to prevent gas condensing. Gas analyses were carried out in Multiple Ion Detection mode (MID) which allows the qualitative determination of evolved masses vs. temperature or time. Background subtraction was performed to obtain the point zero conditions before starting MID analysis.

A synchrotron-based X-ray Absorption Spectroscopy (XAS) technique was used to obtain information on the local chemical environments of Hg-sorbed species. Hg L_{III}-edge X-ray absorption experiments were performed at the European Synchrotron Radiation Facility (ESRF) at GILDA beamline. The monochromator consisted of two Si(311) crystals, and energy calibration was performed using Au-metal foil, with the first inflection point of the L_{III}-absorption edge at 11919 eV. Spectra were collected in transmission mode on powder-pressed disks obtained by mixing an appropriate amount of clay sample with cellulose.

The experimental EXAFS spectrum (χk) is built up from the contribution of the photoelectron waves scattered back from the shells of atoms neighbouring the central atom (Hg) excited by the incident synchrotron radiation. The frequencies of the photoelectron scattered waves can ideally be isolated one from the other using Fourier transformation. After correcting for phase shift effects, each backscattering atom can thus be identified and its distance from the Hg atom calculated by taking into account the intensity and frequency of each elementary wave constituting the EXAFS spectrum. In practice, in real and complex systems the contribution from different backscattered atoms can partially or completely overlap; thus, the Fourier transform spectrum (FT) previously calculated from the EXAFS experimental spectrum was back transformed to generate a Fourier filtered EXAFS spectrum (FT^{-1}).

The Fourier-filtered EXAFS spectrum was compared with theoretical EXAFS spectra, calculated from the FEFF-8 program (Ankudinov et al., 1998). The theoretical spectra referred to structurally well-determined model compounds, which were assumed to present Hg coordinations similar to the sample under examination. The difference between computed and filtered spectra was optimised using a least-squares approach.

To fit the experimental Hg L_{III}-edge spectra was assumed that Hg^{2+} atoms can link water molecules and/or can form oxide and hydroxide precipitates. The experimental spectra obtained for Hg-exchanged montmorillonite and vermiculite were thus fitted using HgO as a reference compound, with the atomic coordinates reported by Wyckoff (1964).

3. Results and discussion

The Hg amount adsorbed confirms the higher affinity of the soft base montmorillonite (37.7 meq Hg/100 g) compared to vermiculite (28.0 meq Hg/100 g). For both clay minerals, the Hg content is below the CEC value, thus indicating a not complete exchange.

At room temperature, the XRD patterns of untreated and Hg-treated samples display the following d_{001} values: (1) montmorillonite sample: $d_{001, untreated} = 15.5$ Å, $d_{001, Hg} = 15.2$ Å; (2) vermiculite sample, $d_{002, untreated} = 14.1$ Å, $d_{002, Hg} = 14.5$ Å. As temperature is increased, the d-value shifts toward 10 Å (Fig. 2). This value is reached at different temperatures (Fig. 2): (1) montmorillonite: untreated sample, $T = 250$ °C; Hg-treated sample, $T = 425$ °C; (2) vermiculite: untreated sample, $T = 300$ °C; Hg-treated sample, $T = 550$ °C.

At temperatures below 400 °C, thermal and evolved gas mass spectrometry analyses of untreated samples suggest that dehydration was complete at
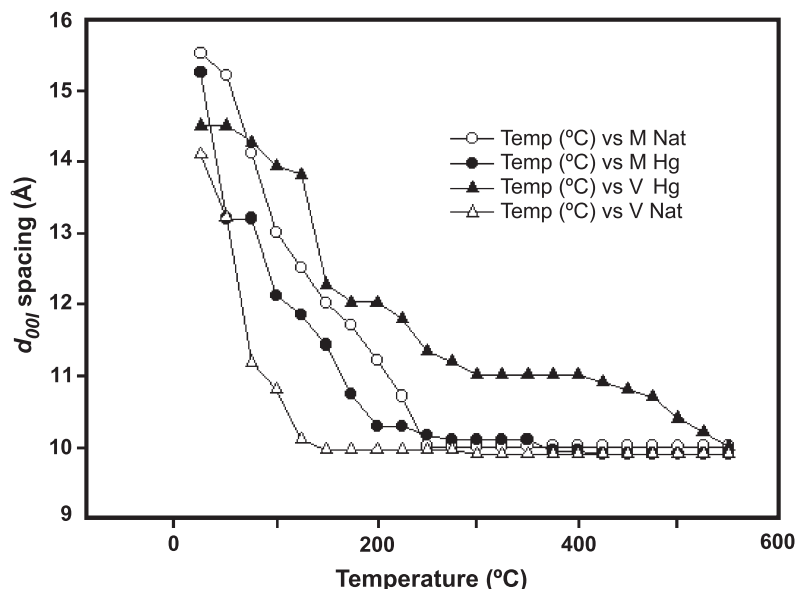

Fig. 2. d_{001} spacing vs. temperature for natural montmorillonite (M Nat), Hg-exchanged montmorillonite (M Hg), natural vermiculite (V Nat) and Hg-exchanged vermiculite (V Hg).

$T<250$ °C both for montmorillonite (Costanzo and Guggenheim, 2001) and vermiculite (vermiculite: endothermic reactions at 102 and 210 °C, weight loss 7.8%). In Hg-treated montmorillonite, the weight loss associated with dehydration (m/z=18) was 8.1% whereas an additional broad endothermic reaction (weight loss 3.1%) was associated with Hg release (m/z=199) (Fig. 3). For Hg-treated vermiculite sample only, reactions associated with dehydration (m/z=18) in the temperature range $25 \leq T$ (°C)≤ 250 (weight loss=7.1%) are identified (Fig. 4). In both samples, the lower weight loss value associated with dehydration can be related to differences of the hydration spheres of Ca^{2+}, Mg^{2+} ions (representing the main interlayer cation of untreated montmorillonite and vermiculite) and Hg^{2+}. Results from thermal analysis confirm these differences in basal spacing as a consequence of the stereochemistry of the interlayer species.

Differences of thermal behavior between Hg-rich montmorillonite and vermiculite also occur at $400<T<1000$ °C. Hg-rich montmorillonite (Fig. 3) shows a weight loss of 4.7% associated with the endothermic reaction at 600 °C, related to simulta-
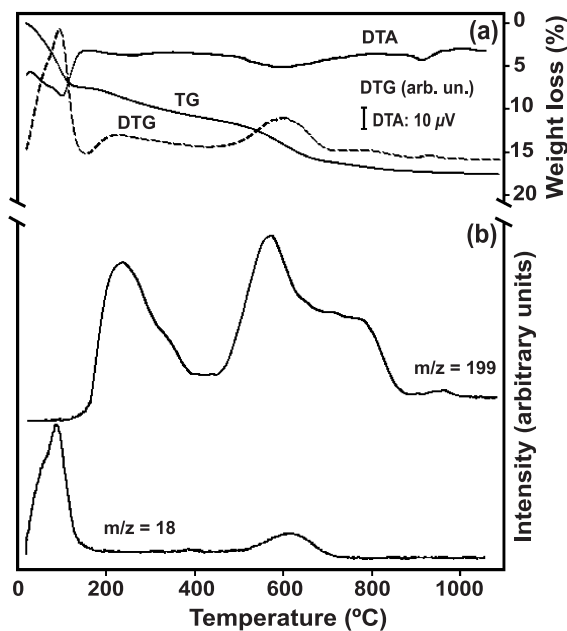

Fig. 3. TG (% weight loss), DTG (weight loss/time), DTA (μV) curves and emitted gas masses of Hg-exchanged montmorillonite. Solid lines represent TG, DTA curves and MS spectra; dashed line represents DTG curves.
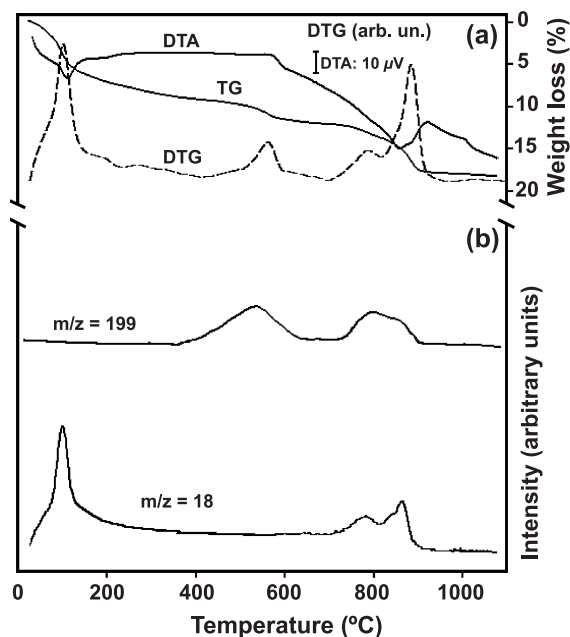

Fig. 4. TG (% weight loss), DTG (weight loss/time), DTA (μV) curves and emitted gas masses of Hg-exchanged vermiculite. Solid lines represent TG, DTA curves and MS spectra; dashed line represents DTG curves.

neous evolution of H_2O (m/z=18) and Hg (m/z=199) and a broad endothermic reaction at about 780 °C (weight loss: 0.8%), due to Hg evolution. The Hg-rich vermiculite (Fig. 4) shows three endothermic reactions at 550, 800, and 860 °C. The reaction at 550 °C is related to Hg evolution (weight loss: 2.6%) whereas the reactions at 800 and 860 °C (weight loss=5.8%) are both linked to 2:1 layer dehydroxylation and Hg emission.

The reaction at 550 °C together with the basal spacing observed for Hg-treated vermiculite at $400 \leq T \leq 550$ °C, reveals the intercalation of Hg–O species. The difference between the basal spacing of Hg-treated vermiculite and those closest packing of the layer (about 10 Å) corresponds to an interlayer separation of about 1 Å. This separation is lower than expected assuming the intercalation of Hg–O polyhedra. Evidently, intercalation occurs in a statistical way.

The FT and the associated FT^{-1} functions generated from the Hg L_{III}-edge EXAFS spectra of Hg-rich montmorillonite and vermiculite are reported in Figs. 5 and 6. A good match was observed in the peak

positions and peak intensities of the experimental spectra of both samples, when compared to HgO (montroydite) as a model compound.

The most relevant contribution to the EXAFS region of montmorillonite (Table 1) was ascribed to Hg surrounded by six oxygen atoms. Three oxygen atoms are closer to Hg, at a distance of 1.99 Å. The distance from Hg of the three remaining oxygen atoms is greater and reaches 2.40 Å. The shorter distances could be interpreted as indicators of Hg–O bonds in montroydite-like compounds, whereas the longer can be ascribed to Hg–O bonds in Hg–H_2O complexes. This latter hypothesis was also formulated by Collins et al. (1999) in studies of a goethite substrate. The lack of symmetry in the Hg coordination sphere is consistent with the two-steps release of the mercury at high temperatures (Fig. 3). The EXAFS analysis also refines two Hg atoms at 3.30 Å from the central Hg atom.

Like in montmorillonite, the vermiculite spectrum is best interpreted in terms of six Hg–O distances with two triads of oxygen atoms at 1.95 and 2.32 Å from the central Hg atom. As described for montmorillonite,

shorter distances are related to Hg–O bond in montroydite-like compounds. Evidence of longer Hg–O distances (2.77 and 2.93 Å) and Hg–Hg distances of 3.31 and 3.37 Å (Table 1) supports the presence of montroydite-like molecules strongly associated to vermiculite. The thermal behaviour shows an evolution of Hg at temperatures higher than in montmorillonite and HgO (Biester et al., 2000), thus suggesting montroydite adsorption into vermiculite interlayers. This conclusion is also supported by the X-ray diffraction (Fig. 2).

4. Concluding remarks

XAS, thermal analyses and mass spectrometry of evolved gas coupled with standard chemical and X-ray diffraction techniques provided useful information on the speciation of mercury ions in montmorillonite and vermiculite.

Results so far obtained underlines that a different layer charge value and charge location greatly affect
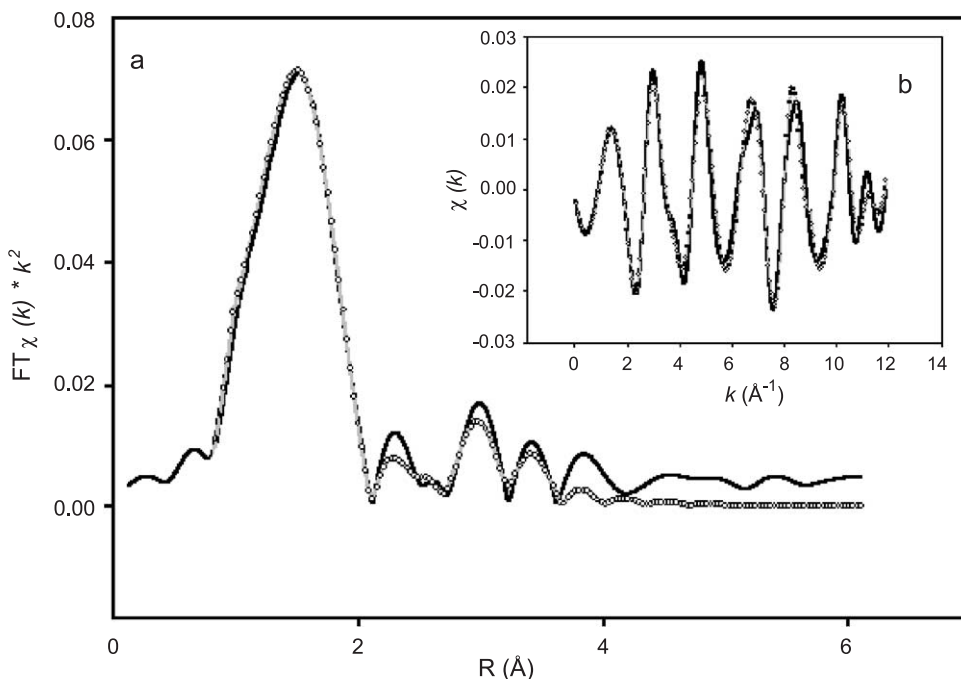

Fig. 5. Hg L$_{III}$-edge EXAFS data for Hg-exchanged montmorillonite. (a) Fourier Transform (FT) and (b) associated inverse Fourier-filtered scattering curve (FT^{-1}) spectra. Solid lines indicate experimental data and circles indicate the fitted curve obtained using HgO as a reference compound.
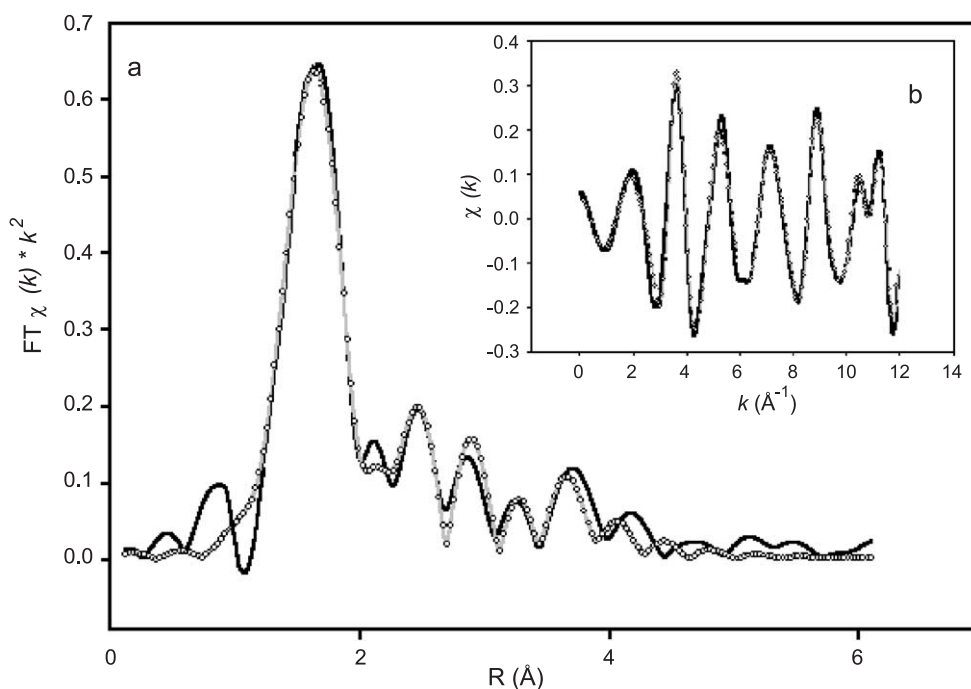
Fig. 6. Hg L$_{III}$-edge EXAFS data for Hg-exchanged vermiculite. (a) Fourier Transform (FT) and (b) associated inverse Fourier-filtered scattering curve (FT^{-1}) spectra. Solid lines indicate experimental data and circles indicate the fitted curve obtained using HgO as a reference compound.

the interaction of the clay minerals with Hg in solution. Montmorillonite is a soft base according to Lewis theory and adsorbs larger amount of Hg, a soft acid, than vermiculite which is classified as a hard base.

The layer charge properties of the mineral affect also the speciation of adsorbed Hg. Hg is preferentially sorbed as Hg–OH$_2$ complexes by montmorillonite and as both Hg–OH$_2$ and Hg–O by vermiculite.

The risk associated to presence of Hg in the natural environment is strongly related to its speciation: Hg–OH$_2$ complexes are less strongly bound to the 2:1 layers, as demonstrated by EXAFS and thermal analysis. On the contrary, Hg–O intercalates are more strongly bounded to the layer and mercury is released at higher temperatures.

Table 1
Result of EXAFS analyses

Hg montmorillonite					Hg-vermiculite				
Aa–Sa	N	R (Å)	σ^2 (Å^2)	ΔE_0	Aa–Sa	N	R (Å)	σ^2 (Å^2)	ΔE_0
Hg–O	3.0	1.99	0.0125	−8.5	Hg–O	2.0	1.95	0.0037	−9.1
Hg–O	3.0	2.41	0.0090		Hg–O	5.6	2.32	0.0100	
Hg–Hg	1.7	3.30	0.0055		Hg–O	1.7	2.77	0.0100	
					Hg–O	2.0	2.93	0.0100	
					Hg–Hg	1.0	3.31	0.0100	
					Hg–O	8.0	3.51	0.0100	
					Hg–Hg	3.7	3.73	0.0100	

Aa–Sa: relationship between central absorber and scattering atom; N: coordination number; R: refined interatomic distance; σ^2: Debye–Waller factor; ΔE_0: energy shift.

References

Allison, J.D., Brown, D.S., Novo-Gradac, K.J., 1991. MINTEQA2/PRODEFA2, A Geochemical Assessment Model for Environmental System: Version 3.0. United States Environmental Protection Agency, Athens, Georgia. 30613.

Allmann, R., 1984. LATCOREF. F.B. Geowissenschaften, Marburg, Germany.

Ankudinov, A.L., Ravel, B., Rehr, J.J., Conradson, S.D., 1998. Real space multiple scattering calculation and interpretation of X-ray absorption near edge structure. Physical Review B 58, 7565.

Behra, P., Bonnissel-Gissinger, P., Alnot, M., Revel, R., Ehrhardt, J.J., 2001. XPS and XAS study of the sorption of Hg(II) onto pyrite. Langmuir 17, 3970–3979.

Biester, H., Gosar, M., Covelli, S., 2000. Mercury speciation in sediments affected by dumped mining residues in the drainage area of the Idrija Mercury Mine, Slovenia. Environmental Science and Technology 34, 3330–3336.

Bothner, M.H., Aruscavage, P.J., Ferrebee, W.M., Baedecker, P.A., 1980. Trace metal concentrations in sediment cores from the continental shelf of the southeastern United States. Estuarine and Coastal Marine Science 10, 523–541.

Collins, C.R., Sherman, D.M., Ragnarsdottir, K.V., 1999. Surface complexation of Hg^{2+} on goethite: mechanism from EXAFS spectroscopy and density functional calculations. Journal of Colloid and Interface Science 219, 345–350.

Costanzo, P.M., Guggenheim, S., 2001. Baseline studies of the clay minerals society source clays. Clays and Clay Minerals 49 (5) (special edition).

Covelli, S., Faganeli, J., Horvat, M., Brambati, A., 2001. Hg contamination of coastal sediments as the result of long-term cinnabar mining activity (Gulf of Trieste-northern Adriatic sea). Applied Geochemistry 16, 541–558.

Donovan, J.J., 1995. PROBE: PC-Based Data Acquisition and Processing for Electron Microprobes. Advanced Microbeam, 4217 C Kings Graves Rd., Vienna, Ohio. 44473.

Gagnon, C., Pelletier, É., Mucci, A., 1997. Behaviour of anthropogenic mercury in coastal marine sediments. Marine Chemistry 59, 158–176.

Haase, O., Klare, M., Krengel-Rothemsee, K., Broekaert, A.C., 1998. Evaluation of the determination of mercury at the trace and ultra-trace levels in the presence of high concentrations of NaCl by flow injection-cold vapour atomic absorption spectrometry using $SnCl_2$ and $NaBH_4$ as reductants. Analyst 123, 1219–1222.

Hudson, R.J.M., Gherini, S.A., Fitzgerald, W.F., Porcella, D.B., 1995. Anthropogenic influences on the global mercury cycle: a model-based analysis. Water, Air, and Soil Pollution 80, 265–272.

Jackson, M.L., 1975. Soil Chemical Analysis, Advanced Course, 2nd ed. University of Wisconsin, Madison Wisconsin. Published by the author. 895 pp.

Kim, C.S., Rytuba, J.J., Brown Jr., G.E., 2004. EXAFS study of mercury(II) sorption to Fe- and Al-(hydr)oxides: II. Effects of chloride and sulfate. Journal of Colloid and Interface Science 270, 9–20.

Lindqvist, O., 1991. Transformation and deposition processes. Water, Air, and Soil Pollution, 55. (Chapter 16).

van Olphen, H., Fripiat, J.J., 1979. Data Handbook for Clay Materials and Other Non-Metallic Minerals. Pergamon Press, Oxford, p. 343.

Watras, C.J., Huckabee, J.W., 1994. Mercury as a Global Pollutant: Towards Integration and Synthesis. Lewis Press, Boca Raton, FL, pp. 203–220.

Watras, C.J., Morrison, K.A., Hudson, R.J.M., Frost, T.M., Kratz, T.K., 2000. Decreasing mercury in Northern Wisconsin: temporal patterns in bulk precipitation and a precipitation-dominated lake. Environmental Science and Technology 34 (19), 4051–4057.

Wyckoff, R.W.G., 1964. Montroydite. Crystal Structures. Wiley Edition, New York. 1, 112.